

INVESTIGATION OF DEUTERON SCATTERING  
FROM  $^{13}\text{C}$  AT LOW ENERGY\*

D.M. JANSEITOV<sup>a,b,c</sup>, N. BURTEBAYEV<sup>a,c</sup>, ZH. KERIMKULOV<sup>a</sup>  
D. ALIMOV<sup>a</sup>, M. NASSURLLA<sup>a,c</sup>, B. MAUYEY<sup>a,b,f</sup>, D.S. VALIOLDA<sup>b,c</sup>  
A.S. DEMYANOVA<sup>d</sup>, A. DANILOV<sup>d</sup>, SH. HAMADA<sup>e</sup>, A. AIMAGANBETOV<sup>f</sup>

<sup>a</sup>Institute of Nuclear Physics, Ibragimova 1, 050032 Almaty, Kazakhstan

<sup>b</sup>Joint Institute for Nuclear Research, Joliot-Curie 6, 141980 Dubna, Russia

<sup>c</sup>al-Farabi Kazakh National University, al-Farabi 71, 050040 Almaty, Kazakhstan

<sup>d</sup>NRC Kurchatov Institute, Akademika Kurchatova pl. 1, 123182 Moscow, Russia

<sup>e</sup>Faculty of Science, Tanta University, Al-Geish, 31512 Tanta, Egypt

<sup>f</sup>L.N. Gumilev Eurasian National University

Satpayev 2, 010008 Nur-Sultan, Kazakhstan

(Received January 7, 2020)

We measured differential cross sections for the elastic scattering of deuterons on a  $^{13}\text{C}$  target using the U-150M cyclotron at INP, Republic of Kazakhstan. The beam energy of deuterons was 14.5 MeV. As a result, we obtained new experimental data for the  $d+^{13}\text{C}$  elastic scattering. Those were combined with literature data and analyzed within the framework of the optical model using the Woods-Saxon and the double folding potentials.

DOI:10.5506/APhysPolB.51.745

## 1. Introduction

Study of elastic and inelastic scattering processes of light charged particles, such as deuterons and  $\alpha$  particles, is one of the main sources of information about the properties of ground and low-lying excited states of nuclei.  $^{13}\text{C}$  is a very interesting nucleus, as it presents various types of structures: the neutron halo in the first excited state at 3.09 MeV ( $1/2^+$ ) [1–3], an analogue of the Hoyle state in  $^{12}\text{C}$  at 8.86 MeV ( $1/2^-$ ) [3, 4], and the recently discovered compact size of the excited state at 9.9 MeV ( $3/2^-$ ) [3, 5, 6]. The main part of these results was obtained based on analysis of experiments of elastic and inelastic scattering [7]. There are only few works, where elastic and inelastic scattering of deuterons from  $^{13}\text{C}$  were studied [8–10].

---

\* Presented at the XXXVI Mazurian Lakes Conference on Physics, Piaski, Poland, September 1–7, 2019.

In this work, differential cross sections of elastic and inelastic deuteron scattering on  $^{13}\text{C}$  were measured at  $E(d) = 14.5$  MeV. Optical-model analyses of the elastic-scattering data were carried out in conjunction with analyses of other  $^{13}\text{C}(d, d)^{13}\text{C}$  differential cross-section data in the energy range of 13.7–18 MeV [8–10]. This paper is a part of our extensive study of the exotic excited states of the  $^{13}\text{C}$  nucleus at low energy.

## 2. Results and discussion

The experimental angular distributions of elastic and inelastic scattering of deuterons from  $^{13}\text{C}$  nuclei were measured using a beam delivered by the U-150M cyclotron at the Institute of Nuclear Physics (Almaty, Kazakhstan) at  $E(d) = 14.5$  MeV within an angular range of 10–100 degrees in the laboratory system.

For optimal focusing of the ion beam on the target, two collimators of 2 mm diameter were used. The  $\Delta E$ – $E$  method was used for detection and identification of reaction products. The telescope detectors consisted of  $\Delta E$  surface-barrier silicon detectors from ORTEC, 50  $\mu\text{m}$  thick, followed by complete absorption  $E$  detectors of 1 mm thickness, used as a stop detector. Thin films of  $^{13}\text{C}$  (isotopic enrichment of about 80%) prepared using electron-beam sputtering were used as targets. During the experiments, several self-supporting films with a thickness of about 150  $\mu\text{g}/\text{cm}^2$  were used. A more detailed description of the experimental setup is given in Ref. [11]. A spectrum of 14.5-MeV deuterons scattered on  $^{13}\text{C}$  at an angle of  $38^\circ$  is shown in Fig. 1.

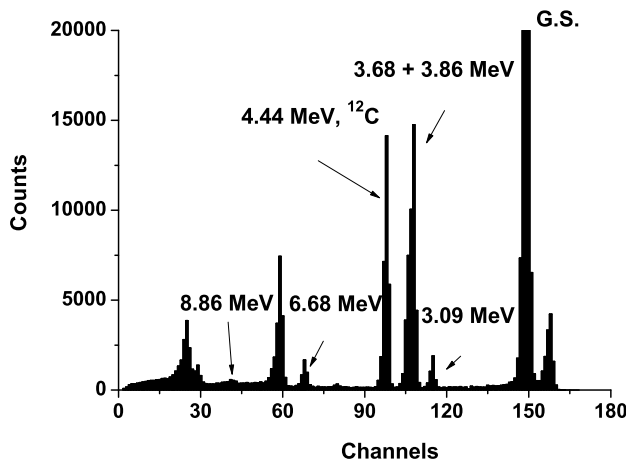


Fig. 1. Typical spectrum of the  $^{13}\text{C}(d, d)^{13}\text{C}$  scattering at the angle of  $38^\circ$ .

Firstly, let us consider the analysis of the elastic scattering cross section. The optical potential was chosen in the usual Woods–Saxon (WS) form and the WS potential consisted of the real and imaginary (with volume absorption) parts. Our total real potential for these cases consists of the nuclear ( $V_{\text{nucl}}$ ), spin-orbit ( $V_{\text{so}}$ ) and the Coulomb ( $V_{\text{C}}$ ) potentials

$$U(r) = V_{\text{nucl}}(r) + V_{\text{so}}(r) (\overline{\mathbf{l}}\mathbf{s}) + V_{\text{C}}(r), \quad (1)$$

where the nuclear potential is assumed to have a Woods–Saxon shape

$$V_{\text{nucl}}(r) = V_0 \left[ 1 + \exp\left(\frac{r - R_v}{a_v}\right) \right]^{-1} + iW \left[ 1 + \exp\left(\frac{r - R_w}{a_w}\right) \right]^{-1}, \quad (2)$$

while the spin-orbit potential is given by

$$V_{\text{so}}(r) = V_0^{\text{so}} \left(\frac{1}{r}\right) \frac{d}{dr} \left[ 1 + \exp\left(\frac{r - R_{\text{so}}}{a_{\text{so}}}\right) \right]^{-1}. \quad (3)$$

Here,  $V_0$  is the WS potential depth,  $R$  the potential radius and  $a$  the diffuseness parameter, which determines the sharpness of the potential surface.

The microscopic nuclear potential that we have also used to analyze the experimental data for the  $d+^{13}\text{C}$  system was based on the double folding (DF) model [12]. The DF potential is calculated by using the nuclear matter distributions of both projectile and target nuclei together with an effective nucleon–nucleon interaction potential ( $\nu_{NN}$ ). Thus, the DF potential is given as

$$V^{\text{DF}}(R) = \int d\mathbf{r}_1 \int d\mathbf{r}_2 \rho_{\text{p}}(\mathbf{r}_1) \rho_{\text{t}}(\mathbf{r}_2) \nu_{NN}(\mathbf{r}_{12}), \quad (4)$$

where  $\rho_{\text{p}}(\mathbf{r}_1)$  and  $\rho_{\text{t}}(\mathbf{r}_2)$  are the nuclear matter density distributions of the projectile and target nuclei, respectively. Gaussian density distributions (GD) were used for the both nuclei [13].

The effective nucleon–nucleon interaction,  $\nu_{NN}$ , is integrated over both density distributions. Several expressions for the nucleon–nucleon interaction can be used for the folding model potentials. We have chosen the most common one, the M3Y (Michigan-3-Yukawa) realistic nucleon–nucleon interaction. The M3Y has two forms, one corresponds to M3Y-Reid [14] and another is based on the so-called M3Y-Paris interaction [15]. In this case, while the real part of the optical model has been obtained by using the above-described DF model, we have adopted the WS form for the imaginary potential.

Therefore, for the nucleon–nucleon-DF potential case, the nuclear potential consists of a real and an imaginary part

$$U^{\text{DF}}(r) = N_r V_{\text{DF}}(r) + iW(r), \quad (5)$$

where  $N_r$  is the normalization factor, which is determined by the fit of the optical model (OM) calculation to the experimental data. Calculations of differential cross sections for elastic scattering were performed within the OM framework using the WS and DF potentials in the FRESKO code [16].

The comparison between the experimental data and the theoretical predictions for  $^{13}\text{C}(d, d)^{13}\text{C}$  at beam energies of 13.7 MeV [8], 14.5 MeV (present work), 17.7 MeV [9] and 18 MeV [10] are shown in Fig. 2. The potential parameters used in the calculations are listed in Table I.

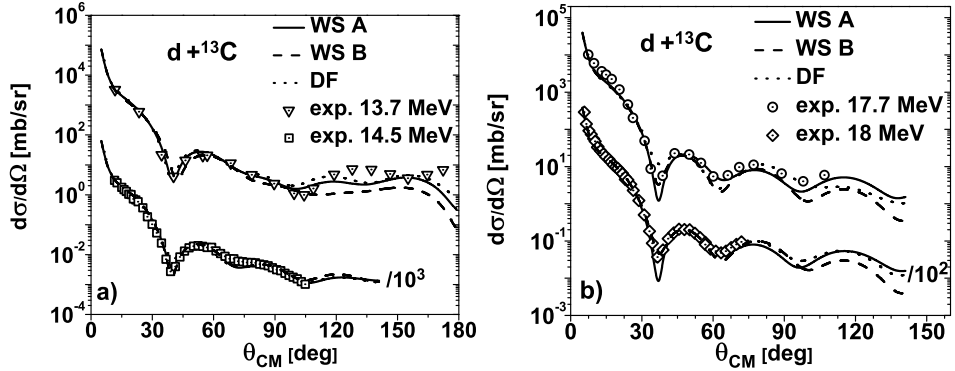


Fig. 2. Comparison between the experimental data and the calculated differential cross section for elastic scattering of deuterons from  $^{13}\text{C}$  at energies 13.7 MeV [8], 14.5 MeV, 17.7 MeV [9] and 18 MeV [10] using WS and DF potentials. The abbreviations WS A and WS B correspond to the calculations of the optical model with a Woods–Saxon potential for different sets of parameters A and B, see Table I. DF corresponds to the calculations of the optical model with a double folding potential for the real part and the imaginary potential taken from WS A.

The global potential of Lohr [17] is taken as the starting potential, but in our case we changed some of its parameters. The standard phenomenological spin-orbit potential is also included in Eq. (3), which allowed improving the description of data at large angles using the following parameters:  $V_{\text{so}} = 9.3$  MeV,  $r_{\text{so}} = 0.9$  fm and  $a_{\text{so}} = 0.9$  fm. To reduce the discrete ambiguity in determining the optical potential (OP), in the WS A calculations the radii of the real ( $r_V$ ) and imaginary ( $r_W$ ) parts and the diffuseness parameters ( $a_V$  and  $a_W$ ) of the potential were fixed. The remaining 2 parameters of OP (namely  $V$ ,  $W$ ) were fitted to the experimental data by  $\chi^2$  minimization. In the WS B calculations, only the radii of the nuclear density distribution for the real ( $r_V$ ) and imaginary ( $r_W$ ) parts of the potential were fixed. In the OM calculations, the Coulomb radius of  $r_C = 1.28$  fm was adopted. The WS B calculations denoted in Fig. 2 by dashed lines are in good agreement with the present experimental data in the full angular

TABLE I

Potential parameters obtained for elastic scattering of deuterons from  $^{13}\text{C}$  at specific energies.

$E$ [MeV]	Set	$V$ [MeV]	$r_V$ [fm]	$a_V$ [fm]	$N_r$	$W$ [MeV]	$r_W$ [fm]	$a_W$ [fm]
13.7	WS A	105.0	1.01	0.80	1.2	8.4	1.8	0.60
	WS B	95.5	1.05	0.85		11.5	1.6	0.60
	DF					8.4	1.8	0.60
14.5	WS A	106.0	0.91	0.80	1.12	12.4	1.8	0.60
	WS B	90.5	1.05	0.83		12.5	1.6	0.50
	DF					12.4	1.8	0.60
17.7	WS A	111.5	0.91	0.80	1.02	9.4	1.8	0.60
	WS B	85.5	1.05	0.88		13.5	1.7	0.54
	DF					9.4	1.8	0.60
18	WS A	113.5	0.91	0.80	1.2	9.0	1.8	0.60
	WS B	85.0	1.05	0.88		13.8	1.8	0.52
	DF					12.4	1.8	0.60

range, while the WS A calculations (solid lines) agree well with experimental points at small scattering angles. This can be explained by the fact that in the case of WS B four parameters of the potential were fitted to experimental data, in contrast to only two for WS A. The main differences between the WS A and WS B sets obtained in this work are the depth and the diffuseness parameters of the real part of the potential.

In the case of DF calculations (dotted lines), the normalization factor ( $N_r$ ) was found to be in the range of 1.01–1.2. Apart from the normalization factor, the imaginary potential parameters were also fitted to the data and the resulting values are listed in Table I. It should be noted that the description based on the DF potential is satisfactory for all energies.

### 3. Summary

We obtained new elastic scattering data using deuteron beams at 14.5 MeV energy incident on a  $^{13}\text{C}$  target. The present data were analyzed using two approaches, namely the phenomenological Woods–Saxon and semi-microscopic double folding potentials. Additionally, we compare our results with experimental data obtained in previous measurements at higher energies.

Inelastic scattering involving excited states, including the 3.09 MeV, ( $1/2^+$ ) state with a neutron halo, the 8.86 MeV ( $1/2^-$ ) analogue of the Hoyle state in  $^{12}\text{C}$ , and the possible compact cluster state at 9.90 MeV ( $3/2^-$ ), was observed, but these data have not been analyzed yet. In future, it is planned to perform analysis of this data using the obtained parameters of optical potentials.

This work was supported by the Russian Foundation for Basic Research (20-32-70115).

## REFERENCES

- [1] T. Otsuka, N. Fukunishi, H. Sagawa, *Phys. Rev. Lett.* **70**, 1385 (1993).
- [2] N. Burtebayev *et al.*, *Int. J. Mod. Phys. E* **27**, 1850025 (2018).
- [3] A.S. Demyanova *et al.*, *Eur. Phys. J. Web Conf.* **117**, 04012 (2016).
- [4] M. Milin, W. von Oertzen, *Eur. Phys. J. A* **14**, 295 (2002).
- [5] A.S. Demyanova *et al.*, *JETP Lett.* **102**, 413 (2015).
- [6] N. Burtebayev *et al.*, *J. Phys.: Conf. Ser.* **1023**, 012025 (2018).
- [7] N. Burtebayev *et al.*, *Int. J. Mod. Phys. E* **25**, 1650078 (2016).
- [8] H. Guratzsch, J. Slotta, G. Stiller, *Nucl. Phys. A* **140**, 129 (1970).
- [9] R.J. Peterson *et al.*, *Nucl. Phys. A* **425**, 469 (1984).
- [10] V.V. Dyachkov *et al.*, *Bull. Russ. Acad. Sci. Phys.* **79**, 89 (2012).
- [11] Sh. Hamada *et al.*, *Phys. Rev. C* **87**, 024311 (2013).
- [12] I.I. Gontchar, M.V. Chushnyakova, *Comput. Phys. Commun.* **181**, 168 (2010).
- [13] M. Karakoc, I. Boztosun, *Phys. Rev. C* **73**, 047601 (2006).
- [14] G. Bertsch *et al.*, *Nucl. Phys. A* **284**, 399 (1977).
- [15] N. Anantaraman, H. Toki, G.F. Bertsch, *Nucl. Phys. A* **398**, 269 (1983).
- [16] I.J. Thompson, *Comput. Phys. Rep.* **7**, 167 (1988).
- [17] J.M. Lohr, W. Haeberli, *Nucl. Phys. A* **232**, 381 (1974).